

Experimental Verification of the Greenhouse Effect

Hermann Harde¹, Michael Schnell²

¹*Helmut-Schmidt-University Hamburg*, ²*Ex Akademie der Wissenschaften Berlin, Germany*

Shortened version of the publication: **Verification of the Greenhouse Effect in the Laboratory**, Science of Climate Change, Vol.1, no 2, p. N4 1-32, 2021, <https://doi.org/10.53234/scc202112//213>

Abstract

We present quantitative measurements for the greenhouse gases carbon dioxide, methane and nitrous oxide under comparable conditions as in the atmosphere and we compare them with radiation transfer calculations. Our experiments allow clear detection of the atmospheric greenhouse effect, at the same time they show its limited influence with growing concentration of these gases.

1. Introduction

Fossil fuel emissions are made responsible for a climate emergency with catastrophic consequences for our planet, when worldwide anthropogenic emissions are not rapidly stopped. The basis of these forecasts is the atmospheric Greenhouse Effect (GHE). However, up to now even many climate experts do not know or understand how greenhouse gases (GH-gases) are affecting our climate. Often this leads to dramatic misinterpretations or exaggerations of the GHE and is spread in this way in popular reviews and even in official publications like the Summary for Policy Makers of the Intergovernmental Panel on Climate Change (IPCC) (Sixth Assessment Report - AR6 [1]). On the other hand, for people with a common sense and/or a critical attitude to unverified theories these exaggerations end in strong doubts about a man-made climate change and the existence of the greenhouse effect, which is almost exclusively based on theoretical considerations.

So, the main reason of these doubts is a missing retraceable verification of the GHE, although there were continuous trials over the last 120 years to confirm or to refute this effect by more or less simple laboratory experiments. Direct measurements at the atmosphere are too strongly affected by convection, turbulence or scattering effects to quantify the relatively small contribution of greenhouse molecules to any local warming of the air or the Earth's surface, which is dominated by day-night and seasonal cycles with local variations of 60°C or more.

It's high time to stop the endless speculations about the disastrous implications or the non-existence of an atmospheric GHE and to concentrate on reliable investigations, which allow to quantify the size but also the limiting impact of GH-gases on global warming caused by anthropogenic emissions of fossil fuels.

The objective of our actual study was therefore to provide clear evidence of the GHE by laboratory measurements and their comparison with calculations, this particularly to refute the often unphysical substitute ideas of GHE opponents, and on the other hand to put into perspective the only moderate influence of GH gases on our climate.

We briefly outline the theoretical background of the GHE and present an advanced experimental set-up, which clearly verifies the GHE under similar conditions as in the lower troposphere. For the first time we present reproducible and quantitative measurements of the back-radiation of the GH-gases carbon dioxide (CO₂), methane (CH₄) and nitrous oxide (N₂O).

The interested reader is referred to the original article (see above) which appeared in the new journal Science of Climate Change.

2. Some Historical Notes

The very first explanation of the atmospheric GHE goes back to Jean-Baptiste Joseph Fourier in 1824 [2], who was studying the Earth's energy budget to explain the surface temperature. He assumed that the atmosphere is acting similar to a glass window, transparent for the solar radiation but blocking the infrared (IR)-radiation emitted from the ground. Heat exchange with the environment by convection or heat conduction was largely neglected in this model.

One of the frontier experimental investigations was performed by R. W. Wood (1909) [3], who used two boxes containing regular air. One box was covered with a glass window transparent for sun light, but blocking IR-radiation, the other covered with a NaCl window transparent also for IR. His measurements showed significant warming of the interior but no or only a negligible temperature difference between the boxes. From this Wood and other authors repeating his experiment (e.g., Allmendinger 2006 [4], Nahle 2011 [5]) concluded that infrared radiation, which can escape through the NaCl window, will not contribute to heating or only with an insignificant amount, while the observed temperature increase in both boxes - different to Fourier's interpretation - is exclusively explained due to the blockage of convective heat transfer with the environment and not related to any kind of trapped radiation.

But experiments recording the temperature at the floor and ceiling of the interior, rather than looking only to a single temperature for each box, measure a 5°C larger floor to ceiling decline for the salt rock box than the glass box, while the bottom of the boxes have almost identical temperatures (V. R. Pratt, 2020 [6]). These results are principally confirmed with a slightly different set-up using an internal electric heating instead of external light sources (E. Loock, 2008 [7]). Such heating avoids differences in the incident radiation, which otherwise has to transmit windows of different materials and losses. A higher temperature of 2.5 - 3°C could be found for the glass box, and replacing the glass by a polished aluminum foil the temperature even rises by additional $\approx 3^\circ\text{C}$.

While the Wood-type experiments can answer the question, if and how far a reduced IR-transmissivity can contribute to warming of a compartment, respectively the troposphere, it gives no information about the interaction of greenhouse gases with IR-radiation. Thus, it still remained the question, to which extent such gases at least partially can withhold IR-radiation and how far simple absorption by GH-gases or the highly disputed back-radiation might contribute to additional warming of the floor. Such studies require to fill one compartment with the gas to be investigated and to compare this with a reference measurement using air or a noble gas.

Meanwhile different approaches have been carried out, partly with external irradiation or with internal heating (Loock [7]), partly measuring the gas temperature or the IR radiation in forward and backward direction (Seim & Olsen 2020 [8]). But either no warming was detected or, after closer inspection, the observed temperature increase could not be attributed to an IR-radiation effect.

Unfortunately some fake demonstrations with apparent temperature differences of more than 10°C are presented in the internet, which allegedly reveal the strong impact of the greenhouse gases (see, e.g., Ditfurth 1978 [9]). However, closer inspection shows that the higher temperature is mainly caused by a stratification effect combined with an increased isolation, when heavier CO₂ is filled from the bottom into the compartment (M. Schnell 2020 [10]). And really problematic is, when the co-recipient of the 2007 Nobel Peace Prize initiates a web-based campaign with multiple advertisements on television, focused on spreading awareness for a climate crisis, and as "evidence" presents a completely unrealistic and unreproducible video experiment of the GHE (Al Gore's Climate 101 video experiment, 2001 [11]), which meanwhile has been falsified by several revisions (Watts 2011 [12], Solheim 2016 [13]). It is a dirty propaganda using such a manipulated experiment to spread fear around the world and to indoctrinate our society with the message that we can only rescue our Earth by stopping all future emissions of greenhouse gases. Such kind of demonstrations undermines any serious attempts to discuss and analyze the expected influence of GH-gases on our climate. Political imaginations, speculations or religious faith are no serious consultants to ensure a prosperous future; our knowledge and technical progress is based on scientific principles.

3. Experimental Set-Up

Fig. 1 displays the experimental set-up that has proven particularly useful for our further investigations. Different to other experiments we use two plates in a closed housing, an upper plate, called earth-plate, which is heated to 30°C, and a cooled plate at the bottom, stabilized to -11.4°C (atmospheric plate, atm-plate). Their distance is 111 cm. No additional light sources in the visible or IR are applied, only the radiation emitted by the two plates and interacting with the gases is considered.

This simulates conditions for the radiation exchange similar to the Earth-Atmosphere-System (EASy) with the warmer Earth's surface and the colder atmosphere. It also avoids any problems caused by an inappropriate spectral range of an external source, which produces a lot of waste heat in the compartment and the windows, but is not well matched to the absorption bands of the GH-gases, and thus significantly reduces the measurement sensitivity.

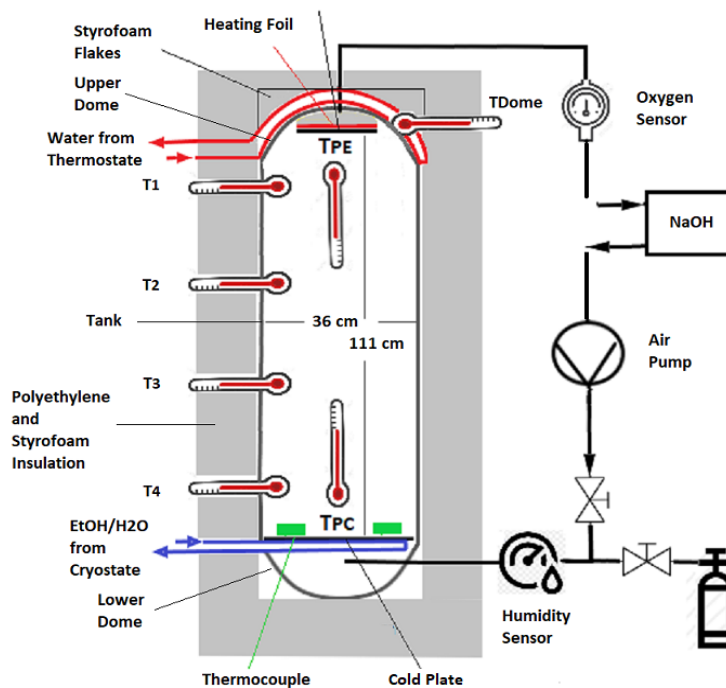


Figure 1: Experimental set-up

With increasing concentration of the GH-gases the radiation balance between the plates is changing and can sensitively be measured as a further increasing temperature of the earth-plate and/or a further cooling of the atm-plate. Here we restrict our investigations on recording the temperature variation of the earth-plate as a function of the GH-gas concentration in the tank, or alternatively controlling the electric power required to stabilize the temperature of this plate to 30°. So, the earth-plate is simultaneously acting as source for IR-radiation and as sensitive detector for the back-radiation from GH-gases.

Any flows, which are not part of the radiation exchange must be prevented or minimized by appropriate measures. The vertical installation, with the earth-plate in the top position, ensures a stable gas stratification during gas injection and prevents vertical heat exchange by convection. Heat conduction, both along the compartment walls or by the gas, cannot be prevented but minimized. This can be achieved with the earth-plate fixed in isolation and located in a hemispheric cover (dome) with almost identical temperature. The dome is wrapped with a vinyl tube on the outside, and water at constant temperature of $30.0 \pm 0.1^\circ\text{C}$ - controlled by an electric heating - flows through this hose. This arrangement is essential for our investigations and ensures that there is almost no heat conduction in this section. So, the heated dome guarantees good thermal insulation of the earth-plate, but is also an important orientation aid for the evaluation of the experiments. It has a polished stainless steel surface, which makes it largely insensitive to thermal radiation.

From the outset, the earth-plate together with the dome has the highest temperature. This results in a small, unavoidable heat flow from the earth-plate to the tank walls and the cold plate, supported by the gases. Any impact of this heat conduction, which inherently is very small, is checked by control measurements with noble gases of comparable heat conductivity and can be excluded.

This set-up allows to reproducibly study the direct influence of GH-gases under similar conditions as in the lower troposphere.

4. Some Theoretical Considerations

4.1 Absorption by GH-Gases

The Earth's surface, or here the black colored earth-plate, can be assumed in good approximation to radiate as black body with a Planck distribution, which is only controlled by the temperature of the body. On a wavelength scale the respective spectrum extends from about 4 μm up to the cm range or in reciprocal wavelengths $1/\lambda$ (unit: wavenumbers per cm) from 10 to 2,500 cm^{-1} . Fig. 2 displays the emitted spectrum of the earth-plate for $T_E = 30^\circ\text{C}$ (Blue Line). Different to nitrogen, oxygen or the noble gases, the GH-gases can absorb radiation in this spectral range.

So, water vapor (WV), CO_2 , CH_4 , N_2O and ozone (O_3) as the main GH-gases in the atmosphere have a total of 615,600 spectral lines in this range, on which radiation can be absorbed. As an example of the radiation interaction with a gas, we consider here CO_2 closer, which alone has 154,500 lines in this range, many of them with only very weak intensity, but over the long absorption path in the atmosphere they also contribute to an absorption of the radiation. The dominating interaction takes place on the ro-vibronic transitions of the CO_2 bending mode around 670 cm^{-1} (15 μm). Plotted in Fig. 2 is the calculated spectral intensity transmitting a gas sample of 20% CO_2 in dry air at a constant temperature of 20°C and over a distance of 111 cm (Plum colored). This calculation is based on the Lambert-Beer law and shows complete opacity around the band center (Yellow Area), while the semi-transparent wings (Gray) together with the weak bands around 1,000 cm^{-1} and 2,100 cm^{-1} are only partly contributing to a further slowly increasing absorption with inclining CO_2 concentration. In the atmosphere with a CO_2 -concentration of 410 ppmv and neglecting interference with water vapor lines this corresponds to an atmospheric layer thickness of 540 m.

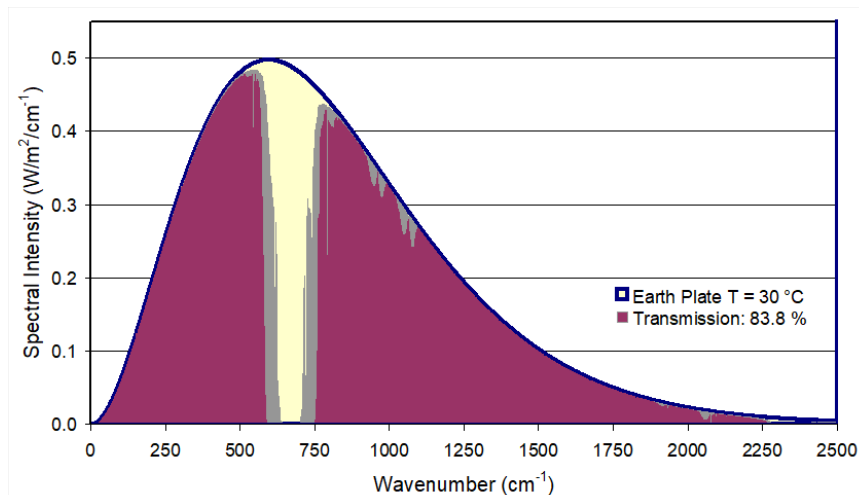


Figure 2: Spectral intensity radiated by the earth-plate at $T_E = 30^\circ\text{C}$ (Blue Graph) as a function of wavenumbers. Transmission of initial radiation through 20% CO_2 in dry air at a temperature of 20°C and over a pathlength of 111 cm is shown in Plum color.

The absorbed radiation by the gas is in a first step converted into local heating, but all this does not take into account any re-emission of the gas, which is superimposing the incident radiation and significantly changes the observed radiation and energy balance.

4.2 Thermal Emission of a GH-Gas

One of the most common objections against the GHE is that GH-gases would not emit in the lower atmosphere, while they are good emitters in the tropopause and stratosphere. As explanation critics state that in the lower troposphere collision processes with nitrogen and oxygen suppress any spontaneous emission and the absorbed energy is only converted into kinetic energy and thus into heat via collisions.

Unfortunately such interpretation overlooks that the typical collision rates of several GHz, as they are observed in the lower atmosphere, are only reducing by a factor of 4 - 5 at an altitude, e.g., of 11 km and therefore are still some 100 million times larger than the spontaneous transition rate on the CO₂ bending mode (~1 Hz). When such interpretation would be true, there would also be absolutely no emission in the higher atmosphere.

Continuous emission even without prior absorption of an IR light quantum occurs mainly, because in addition to superelastic collisions (collision-induced transition from a higher to a lower molecular state) also inelastic collisions take place, which remove kinetic energy from the gas mixture and convert it back to excite GH-gas molecules (Harde 2013 [14], Subsec. 2.3). Thus, lower-lying energy levels are continuously re-populated, when there is sufficient thermal energy, and spontaneous emission occurs largely independently and parallel to the superelastic collisions as thermal background radiation (Harde 2013 [14], Subsec. 2.5). Collisions (adiabatic and diabatic collisions) are primarily noticeable as spectral broadening of the lines. But on these frequencies and over longer pathlengths the radiation can achieve the same strength as a blackbody radiator, and at thermal equilibrium this is only controlled by the gas temperature T_G .

Next to a reduced gas density this temperature is the main reason that with increasing altitude the radiated intensity is significantly decreasing. So, at an altitude of 11 km for CO₂, e.g., it is just 12% of the intensity observed in a 100 m thick gas layer close to the ground.

A complete and realistic description of a measurement with the presented apparatus therefore requires that this emission, which occurs in the same spectral range as the earth-plate radiation and can significantly reduce the effective absorption losses, is included. Respective calculations considering a continuous absorption-emission sequence for propagating radiation in a gas is known as Radiation Transfer calculation (RT-calculation, Schwarzschild equation) (Harde 2013 [14], Sec. 4).

In particular, from such calculation follows:

- For a GH gas that has the same temperature as an external Planck radiator, here the earth-plate, the transmitted radiation is equal to the incident radiation. Changes can only be expected, when T_E and T_G are different and/or T_G varies over the pathlength.
- This already explains, why it is difficult to verify the GHE when only looking to the gas temperature. Net absorption and thus heating of the gas by incident radiation only takes place as long as the respective spectral intensity on the molecular transitions is larger than the eigen-radiation of the gas on these lines. When this has equalized, no further net exchange happens, and in this sense RT in the gas acts similar to heat conduction and convection equalizing local temperature differences.
- A larger local and global warming of a GH-gas is also restricted by its own radiation. This limits the effective absorption from an IR or visible light source and impedes distinction of this contribution from the dominating waste heat released by these sources. All this is further aggravated in the presence of heat conduction and convection in a typical set-up.
- A prerequisite for the observation of the GHE in the atmosphere and in the same way in a laboratory experiment is a temperature gradient in the gas, otherwise no net changes in the radiation balance can be expected.

4.3 Forward-Radiation

Fig. 3 shows a Line-By-Line-Radiation-Transfer (LBL-RT) calculation for 20% CO₂ in air over 111 cm. But different to Fig. 2 varies the gas temperature over the propagation length from 30°C at the earth-plate to -11.4°C at the cooled plate. This corresponds to a lapse-rate of 0.373°C/cm over the gas column. The emitted radiation of the earth-plate is indicated as Blue graph on a yellow background, the transmitted spectral intensity in front of the cold plate is displayed in Plum, and the weak absorption bands as well as the semitransparent wings are plotted in Grey. The significantly lower absorption with 5.2% compared to Fig. 2 with 16.2% is obvious and is the result of the eigen-emission of the gas.

This calculation was performed by balancing stepwise the absorption and emission over a layer thickness of $\Delta z = 1$ cm. For each layer the spectral changes of more than 12,000 lines with their pressure and temperature dependent linewidths have to be calculated to finally derive the transmitted intensity after 111 calculation steps. The pressure in the tank was assumed to be constant and the gas density considered to change according to the ideal gas equation.

Fig. 3 reproduces conditions as recorded by satellites measuring the upwelling radiation or forward scattering, which is characterized by the typical funnel around 670 cm⁻¹. In this spectral range is the incident radiation completely absorbed (see Fig. 2), and the observed intensity only results from thermal emission of the gas at reduced temperatures close to the lower plate. In this case the gas first absorbs 73.6 W/m² from the incident radiation of 479 W/m² (integral over the spectral intensity) and emits again 48.5 W/m², while a difference of 25.1 W/m² remains in the gas volume and can contribute to warming and/or radiation, as long as this is not lost at the walls.

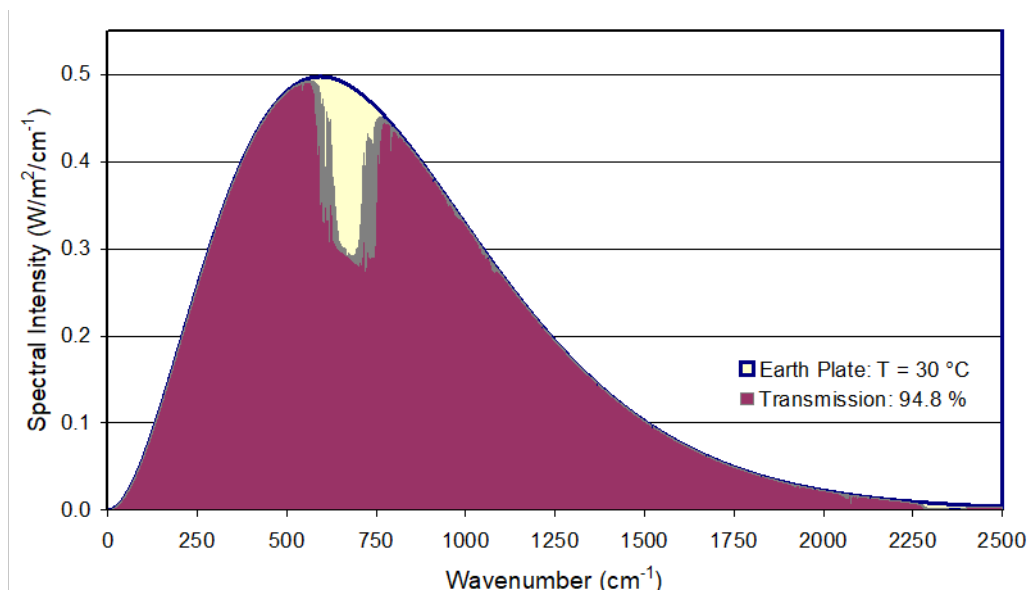


Figure 3: LBL-RT-calculation for 20% CO₂ in air over 111 cm for a lapse rate of 0.373°C/cm. Plotted is the blackbody radiation for 30°C (Blue-Yellow) and the transmitted spectral intensity (Plum-Gray).

To detect the forward or upwelling radiation is one way to verify the GHE, the other approach, we prefer in this contribution, is to measure the downwelling or backward radiation. In analogy to the terrestrial radiation we define the propagation from the warmer to the colder plate as positive z-direction and as upwelling radiation, although our set-up is just upside-down to EASy.

4.4 Radiation of the Atmosphere Plate

A full radiation balance not only has to consider the emission of the earth-plate and the interaction with the gas but also the radiation emitted by the cold plate, which is propagating in anti z-direction through the gas towards the warmer plate.

Again there are objections from GHE opponents who argue that the radiation from a cooler body cannot be absorbed by a warmer body, as this would violate the 2nd law of thermodynamics. A simple measurement, in which the temperature of the atm-plate is gradually increased and the warming of the earth-plate or its reduced heating capacity is measured, is clear evidence of a wrong interpretation of this law, which explicitly includes "simultaneous double heat exchange by radiation" (Clausius). In a closed system, "the colder body experiences an increase in heat at the expense of the warmer body," which in turn experiences a slower rate of cooling. In an open system with external heating, the back-radiation from the colder body clearly leads to a higher temperature of the warmer body than without this radiation.

Fig. 4 shows such a measurement for the heating or the saved heating intensity (to stabilize the earth-plate at $T_E = 30^\circ\text{C}$) as a function of the radiation intensity I_A of the atm-plate (Magenta). The linear progression confirms an almost exclusive radiation transfer according to the Stefan-Boltzmann law, while heat conduction or convection can be largely ruled out.

Likewise, the radiation loss caused by divergence and reflection at the side walls can be determined from such a measurement. It results in a transmission factor f_A of about 74%. For comparison, the graph without losses is shown (Blue). At the same time, the reduced heating at an observed temperature increase provides a calibration for the temperature response sensitivity of the earth-plate with $\lambda_E = 0.083 \text{ }^\circ\text{C}/\text{W}\cdot\text{m}^2$.

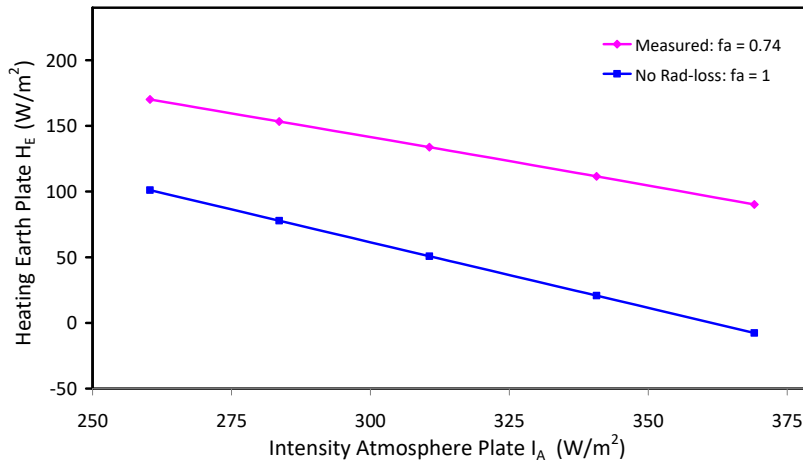


Figure 4: Measured heating of earth-plate for a fixed temperature T_E of 30°C as a function of the radiated intensity I_A of the atm-plate (Magenta Diamonds). Also plotted is the expected heating for $f_A = 1$ (Blue Squares).

4.5 Back-Radiation

When radiation from the atm-plate is propagating through the gas towards the warmer plate, just opposite to Fig. 3 the gas emission is increasing over the pathlength and the spectral components within the CO_2 -absorption band are now further 'amplified'. Fig. 5 shows the transmitted spectral intensity (Plum Area) emitted by the atm-plate (at $T_A = -11,4^\circ\text{C}$, Blue Line) and the gas cloud at 20% CO_2 in dry air over 111 cm. The additional emission of CO_2 can well be identified as a larger peak around 670 cm^{-1} (Plum-Gray). On the stronger lines at the band center the gas emission already attains saturation with spectral intensities, which are the same as those emitted by the earth-plate (Red Line) in this spectral range.

Compared to the total radiated intensity of the atm-plate with $I_A = 266 \text{ W}/\text{m}^2$ the back-radiation increases by $24.2 \text{ W}/\text{m}^2$, which is 9.1%. This larger back-radiation is almost identical to the losses in forward direction, so that within observational accuracies the total balance of absorption and emission of the gas is zero. This is a further important aspect that speaks against measuring the gas temperature to prove the GHE. On the other hand, with the set-up presented in Section 3, the back-radiation of the GH-gases can well be detected through a temperature rise of the earth-plate.

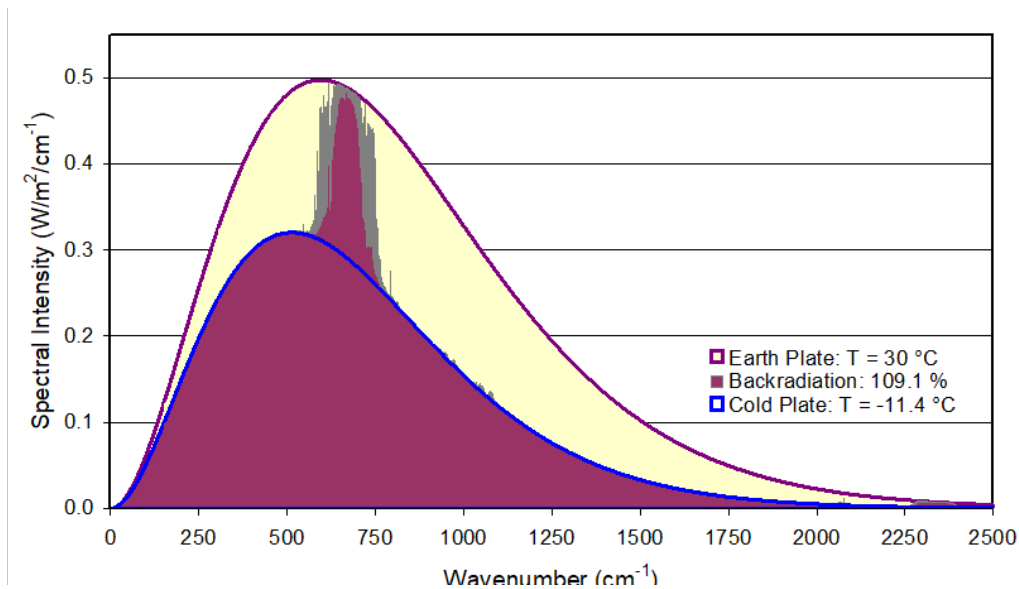


Figure 5: LBL-RT-calculation for 20% CO₂ in air over 111 cm for a lapse rate of -0.373°C/cm: Back-radiation from cold plate and gas (Plum-Gray), radiation only from cold plate (Blue) and spectral intensity of earth-plate (Red-Yellow).

5. Measurements

We have investigated the GH-gases CO₂, CH₄ and N₂O over a wide range of concentration changes up to a factor of 16. For all measurements the temperature of the cold plate is -11.4°C and not changed over a run. In a preparatory phase, the electric heating H_E of the earth-plate is adjusted, till the temperature of the earth-plate is exactly 30.0°C. Before adding a GH-gas to the chamber, all components of the setup must come to thermal equilibrium, as controlled by temperature measurements taken during the first 60 minutes before the sample gas is added. The accuracy of the temperature reading is $\pm 0.13^\circ\text{C}$, which can further be increased by independent measurements and averaging over several runs.

Fig. 6 displays a typical plot, in this case for 10% CO₂ over the full recording time. The different graphs indicate the measured temperatures for the earth-plate (Red), the dome (Green), the gas at different positions of the chamber ($T_1 - T_4$, see Fig. 1) and the laboratory (Black).

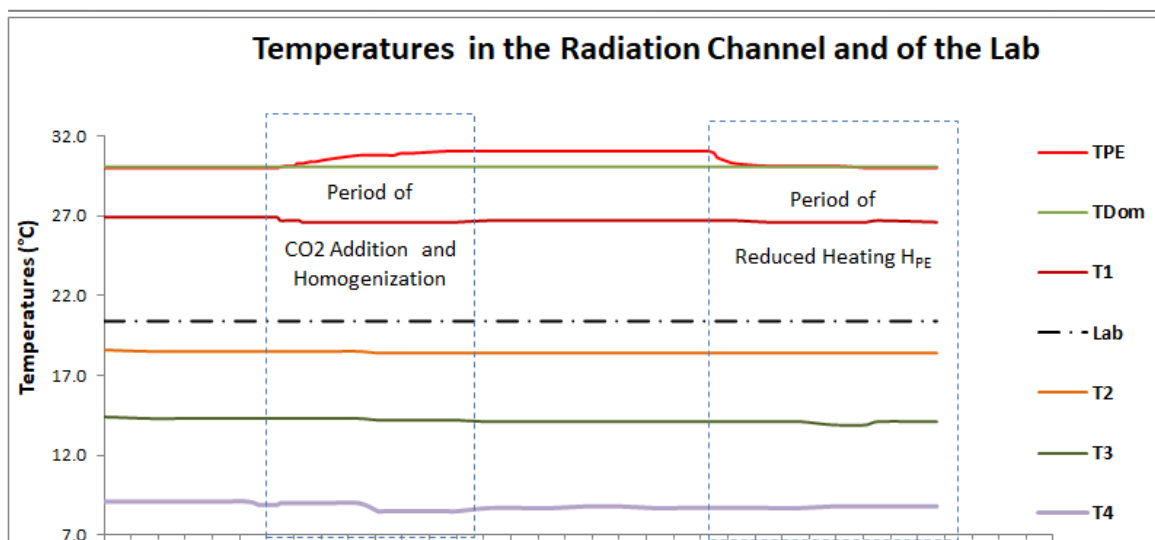


Figure 6: Typical measurement cycle, here for 10% CO₂ in dry air. Plotted are the temperatures of the earth-plate (Red), the dome (Green), the gas temperature at 4 positions $T_1 - T_4$ (see Fig. 1) and the laboratory temperature (Black).

After filling the tank with a GH-gas a new equilibrium and constant temperature increase ΔT_E of the earth-plate has established within one hour. Then the electric heating is reduced to return to 30°C at the earth-plate, allowing a direct measurement of the back radiation as difference of the required electrical heating ΔH_E of the earth-plate.

5.1 CO₂-Measurement

Fig. 7a displays the measured temperature increase ΔT_E at the earth-plate as a function of the CO₂-concentration, which was stepwise increased from 1.25% up to 20% (Blue Diamonds).

As direct comparison is also plotted the calculated temperature increase $\Delta T_E = \lambda_E f_{CO_2} \cdot \Delta I_{CO_2}$ (Magenta Squares), based on an RT-calculation of the changing CO₂ back-radiation ΔI_{CO_2} (Green Triangles), only multiplied by a calibration factor (transmitted fraction) f_{CO_2} for the collected radiation (see below) and the separately measured temperature response λ_E of the earth-plate. The temperature variation ΔT_E can well be represented by a logarithmic curve of the form:

$$\Delta T_E(C_{CO_2}) = \Delta T_0 + \lambda_{av} \cdot f_{CO_2} \cdot \Delta F_{2xCO_2} \cdot \ln(C_{CO_2} / C_0) / \ln 2, \quad (1)$$

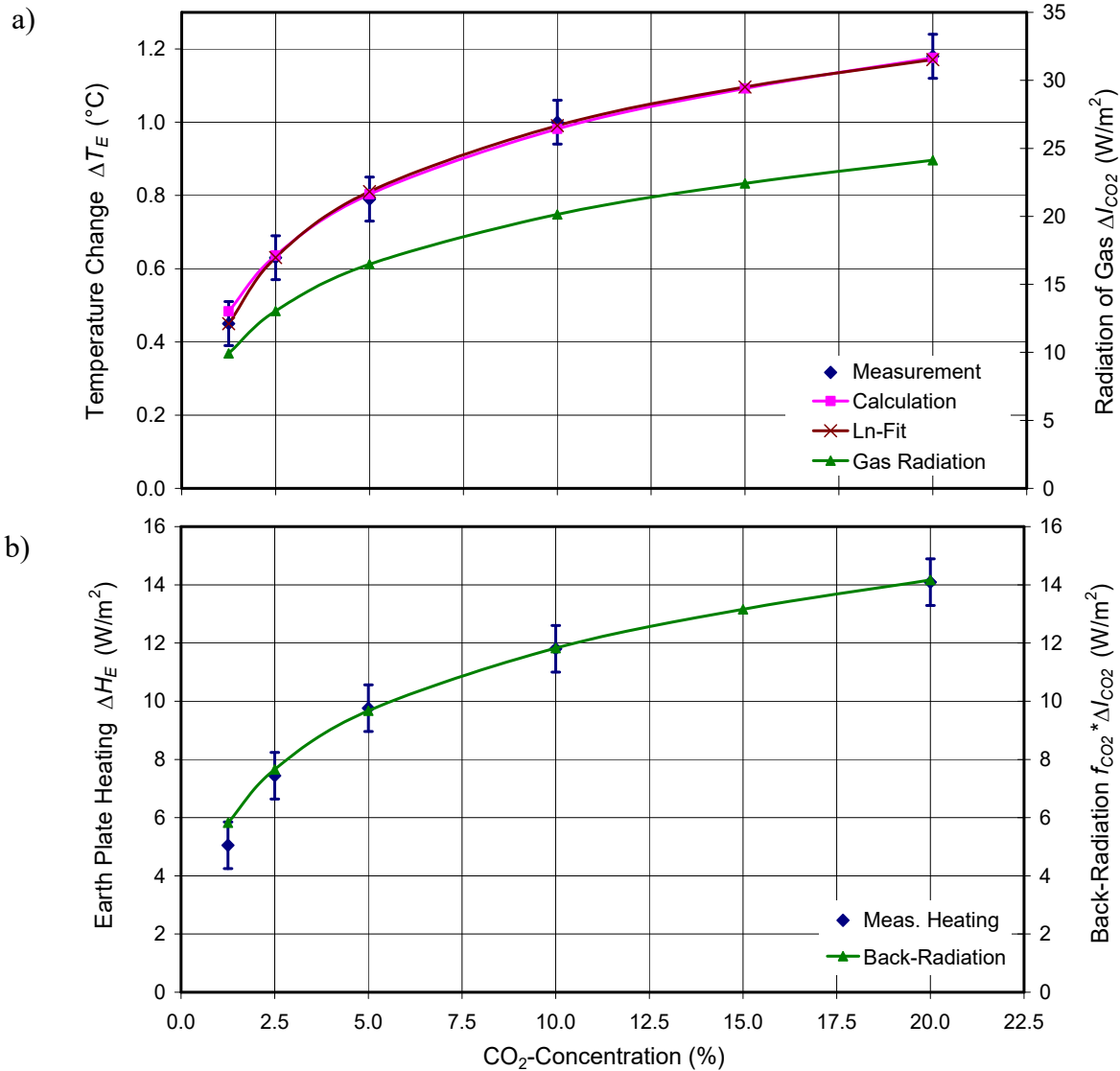


Figure 7: a) Measured temperature change of the earth-plate as a function of the CO₂-concentration in dry air (Blue Diamonds) and calculation (Magenta Squares). Superimposed is a logarithmic fit (Brown Crosses) and the LBL-RT-calculation of the back-radiation ΔI_{CO_2} . b) Comparison of measured plate heating ΔH_E (Blue Diamonds) and calculated back-radiation collected by the earth plate $f_{CO_2} \cdot \Delta I_{CO_2}$ for $f_{CO_2} = 0.59$ (Green).

with ΔT_0 as the temperature increase at the concentration C_0 , here 1.25%, and $\Delta F_{2\times CO_2}$ as radiative forcing when doubling the CO_2 concentration. Superimposed in Fig. 7a is a fit based on (1) with $\Delta F_{2\times CO_2} = 3.70 \pm 0.05 \text{ W/m}^2$ (Brown Crosses), which on first glance shows excellent agreement with the literature, but is derived under different conditions (see Sec. 6).

The measured plate heating variation ΔH_E as an independent means for detecting the back-radiation is plotted in Fig. 7b (Blue Diamonds). Multiplied with the temperature response λ_E of the earth-plate this again reproduces the measurement displayed in Fig. 7a. ΔH_E can also directly be compared with the calculated back-radiation $f_{CO_2} \cdot \Delta I_{CO_2}$ (Green Triangles) with f_{CO_2} as the free parameter for a fit to the measurements. From this fit we derive the fraction $f_{CO_2} = 0.59$ of the emitted gas intensity absorbed by the plate.

5.2 CH₄-Measurement

Measurements for CH₄ were performed for concentration changes from 1.25 to 10% in dry air. The observed temperature increase ΔT_E of the earth-plate as a function of the CH₄ concentration (Fig. 8, Blue Diamonds) shows again excellent agreement with the calculated temperature increase (Magenta Squares) based on the calculated back-radiation ΔI_{CH_4} (Green Triangles).

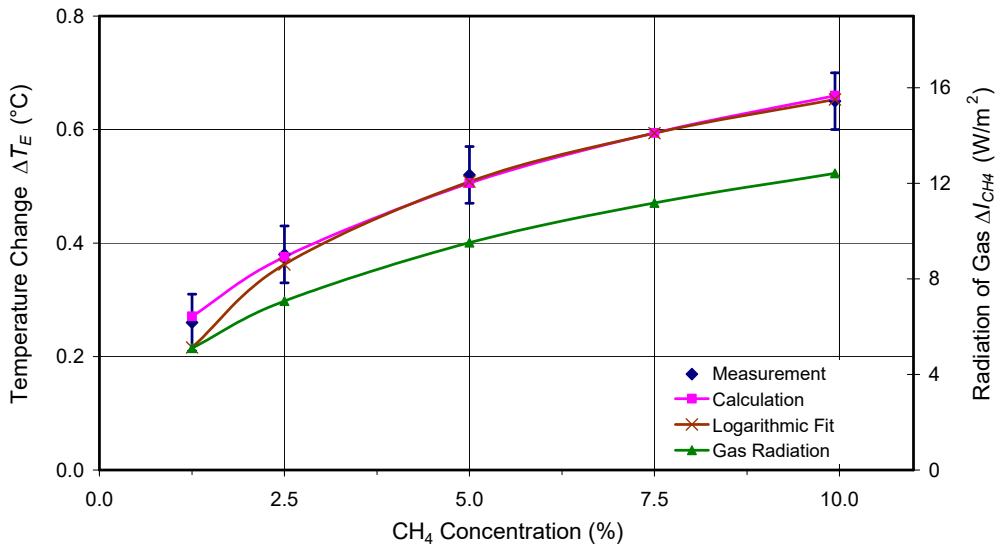


Figure 8: Measured temperature variation of the earth-plate as a function of the CH₄-concentration in dry air (Blue Diamonds) and calculation (Magenta Squares). Superimposed is a fit assuming a logarithmic function (Brown Crosses) and the LBL-RT-calculation of the back-radiation ΔI_{CH_4} (Green Triangles).

Except for the lowest concentration also this GH-gas indicates strong saturation at these concentration levels and can quite well be represented by a logarithmic plot (Brown Crosses) with a radiative forcing at doubled CH₄ concentration of $F_{2\times CH_4} = 2.75 \text{ W/m}^2$. Under otherwise comparable conditions this is only 74% of the CO₂ forcing. Although the atmospheric concentration of CH₄ with 1.8 ppm is more than 200x smaller than CO₂, over the optical path - proportional to the concentration x propagation length - also CH₄ shows stronger saturation in the atmosphere.

5.3 N₂O-Measurement

The N₂O measurements were performed for concentrations of 1.25% up to 15%. The recorded temperature change ΔT_E of the earth-plate with increasing N₂O concentration (Fig. 9, Blue Diamonds) can again well be reproduced by the calculated change $\Delta T_E = \lambda_E f_{N_2O} \cdot \Delta I_{N_2O}$ (Magenta Squares). The theoretical N₂O emission ΔI_{N_2O} is shown as Green Triangles.

The measured temperature also fits well to a logarithmic curve (Brown Crosses) and gives an N_2O radiative forcing at doubled concentration of $\Delta F_{2xN_2O} = 5.0 \text{ W/m}^2$, which is 35% greater than the CO_2 forcing.

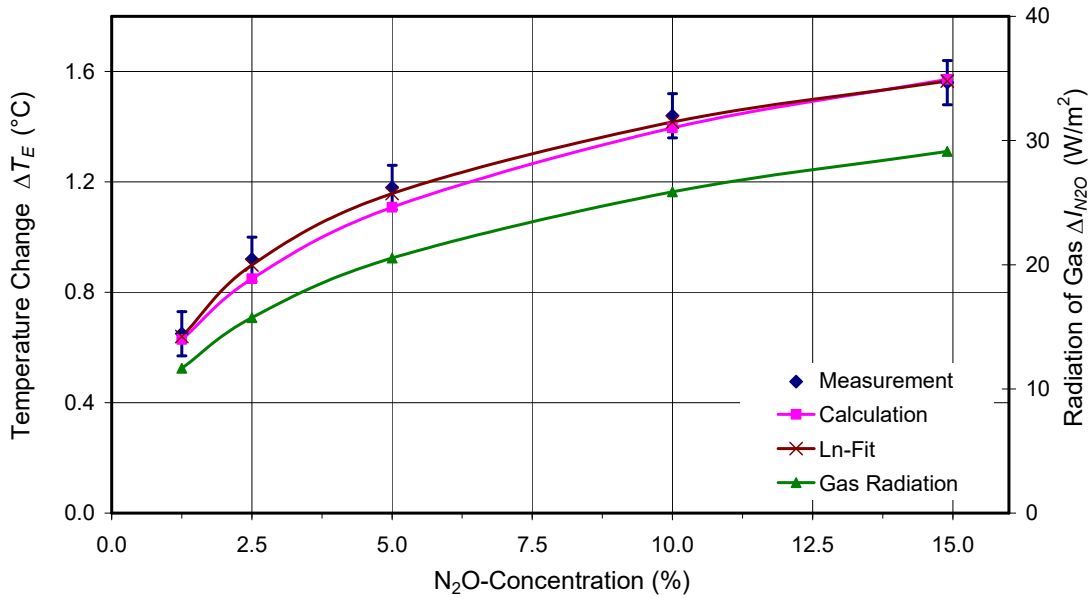


Figure 9: Measured temperature change of the earth-plate as a function of the N_2O -concentration in dry air (Blue Diamonds) and calculation (Magenta Squares). Superimposed is a fit with a logarithmic function (Brown Crosses) and the LBL-RT-calculation of the back-radiation ΔI_{N_2O} (Green Triangles).

6. Discussion of Results

6.1 Differences to Atmospheric Conditions

The experimental set-up as presented in Section 3 has proven to be appropriate for demonstrating the atmospheric GHE in the laboratory. Although the pathlength through the atmosphere is about a factor of 80,000 larger than in the tank, this is partially compensated by a 500x higher concentration for CO_2 , a 50,000x larger CH_4 -concentration, and it is even significantly overcompensated for N_2O with an almost 500,000x higher concentration relative to the sea-level values. Not so much the absolute values are relevant, more important is the optical depth, which scales with the absorption coefficient of the gases \times pathlength.

On the other hand is the lapse rate over the troposphere with $6.5^\circ\text{C}/\text{km}$ 5.700x smaller than in our experiment, while the absolute temperature difference is almost comparable.

But most important for the verification of the GHE and the back-radiation from IR-active gases is their emission in the presence of collisions, and this under conditions as found in the lower troposphere. The experiments definitely confirm that GH-gases are radiating on their transitions, and within an optically thick layer even comparable to a black-body radiator with the same temperature as the gas.

6.2 Impact of Background Radiation

Under real atmospheric conditions is the back-radiation of the GH-gases superimposed by the much broader radiation from clouds, which in first approximation can be assumed as grey emitters with an emissivity < 1 and a temperature determined by the bottom side of the clouds.

In our experiment clouds are represented by the atm-plate and walls, and additionally to the GH-gas emission also this radiation is absorbed by the earth-plate. This total back-radiation is strongly

changing with the temperature of the atm-plate T_A (see Fig. 4) and in this way simulates the impact of clouds at different heights, and thus temperatures. But it also affects the size of the GH-gas contribution, which depends on the temperature difference between the plates and by this on the lapse-rate. Transferred to the atmosphere this means that with clouds the back-radiation is larger than for clear sky, but the relative contribution caused by GH-gases is declining.

6.3 Reproducibility and Accuracy

The reproducibility of the measurements is strongly dependent on the equilibrium conditions of the whole equipment when recording the data. The temperature reading is limited to $\pm 0.13^\circ\text{C}$, and thus, essentially determines the accuracy of the measurements. Also the electric plate heating is affected by the temperature reading, as any initial and final tracing to derive the difference ΔH_E , requires two temperature measurements. The room temperature is controlled within $\pm 0.2^\circ\text{C}$.

The error for an individual measurement of the temperature increase ΔT_E and the reduced plate heating ΔH_E we estimate as $\pm 20\%$ at the lower concentrations and as about $\pm 10\%$ at the higher concentrations. However, the overall accuracy can further be improved by repeating the measurements several times. All presented data are the average of 5 independent runs. This allows to determine the general trend of a series well within $\pm 5\%$.

6.4 Comparison with Theory

For a direct comparison of the measurements with a calculation the key parameters are the temperature sensitivity λ_E and the fraction f_G of the emitted gas intensity ΔI_G which is absorbed at the earth-plate. While λ_E can directly be deduced from the slope of the measured temperature increase as a function of the electric heating, f_G as the ratio of $\Delta H_E/\Delta I_G$ is derived from a fit of ΔI_G to ΔH_E as shown in Fig. 7b for CO_2 . A completely independent means to determine f_G and thus the radiative forcing $\Delta F_{2\times G}$ would require a known volume radiator as reference. While the transmitted fraction f_A from the atm-plate can work as a first orientation, here we are using a theoretical reference, the calculated emission of the gas itself.

For all three gases we find good agreement between measurement and calculation, this for the temperature data as well as for the plate heating. Particularly the increasing saturation and the characteristic gradation with inclining gas concentration is well confirmed by the calculations and excludes any larger impact by heat conduction. At the same time these graphs demonstrate the only small further impact on global warming with increasing GH-gas concentrations.

While the coincidence in the absolute values of measured and calculated data is a consequence of using the theoretical reference for deriving f_G as scaling factor for the absorbed back-radiation and the temperature plots, is the almost exact agreement of the derived radiative forcing for CO_2 with $\Delta F_{2\times\text{CO}_2} = 3.70 \text{ W/m}^2$ more an unexpected coincidence with the literature (see AR6 [1]), as the measurement here was deduced under quite different conditions. in (1)

A comparable Earth-atmosphere scenario to our experiment would be a surface temperature of $T_E = 30^\circ\text{C}$, a dense cloud cover at about 5,200 m altitude, a CO_2 concentration of 42.7 ppm and no other GH-gases. The cloud cover at this altitude then has a temperature of -11.4°C and radiates with 266 W/m^2 (assuming 100% emissivity), while the reduced CO_2 concentration over a pathlength of 5.2 km ensures a comparable optical path to the experiment ($20\% \times 1.11 \text{ m}$). A simulation under these conditions almost reproduces the measurement with a CO_2 induced back-radiation of 23.5 W/m^2 and a radiative forcing for doubling the concentration from 21.35 ppm to 42.7 ppm of $\Delta F_{2\times\text{CO}_2} = 3.74 \text{ W/m}^2$. This already includes a first smaller correction due to the declining pressure with altitude, and thus a lower collisional broadening, which reduces the forcing by about 0.2 W/m^2 , while the pressure in our measurement and calculation was considered to be constant.

A much larger impact on the back-radiation and the radiative forcing, however, emanates from other GH-gases in the atmosphere, particularly from water vapor. So, under conditions as above and assuming only about one tenth of the regular concentration of H₂O, CH₄ and N₂O (to preserve the ratio to CO₂), the back-radiation increases by 80 W/m², while the CO₂ induced forcing decreases by 1 W/m² to 2.71 W/m² (Fig. 9).

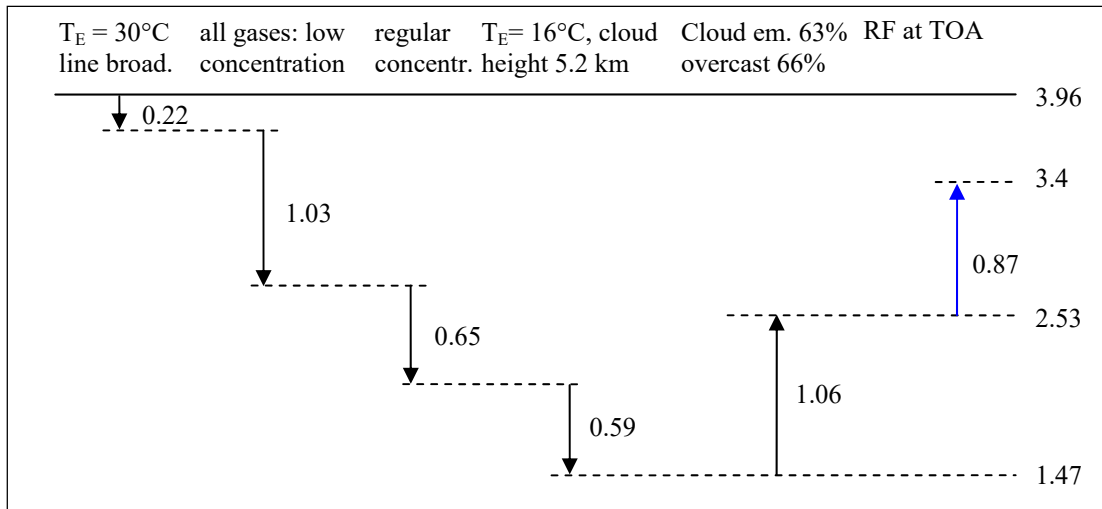


Figure 10: Changes of radiative forcing ΔF_{2xCO_2} in W/m² caused by different impacts. Black arrows indicate changes in back-radiation, blue arrow in forward radiation at TOA.

When repeating the above calculation with the actual concentrations of the GH-gases (CO₂: 400 ppm; H₂O: 1.46%; CH₄: 1.8 ppm; N₂O: 0.3 ppm), the back-radiation further increases to 418 W/m², which is already 87.5% of the up-welling surface emission (478 W/m²), but due to the strongly overlapping and saturated absorption bands the forcing even reduces to $\Delta F_{2xCO_2} = 2.06$ W/m². For a ground temperature of 16 °C it further goes down to 1.47 W/m².

A more realistic scenario with a global mean Earth temperature of 16°C, a mean cloud cover of 66% and a cloud emissivity of 63% increases the forcing by 1.06 W/m², and when finally calculating the forcing at the top of the atmosphere (TOA) for doubling the concentration from pre-industrial times with 280 ppm to 560 ppm, this gives a value of $\Delta F_{2xCO_2} = 3.4$ W/m². So, this must be seen more as a coincidence, when our measurement almost reproduces this measure with its different impacts, which even partly compensate each other. Nevertheless is this an important orientation, and both the back-radiation by CO₂ and the almost logarithmic variation of the radiative forcing with concentration changes, as expected from the calculations, can well be confirmed by our measurements. With a Planck response of $\lambda_P = 0.31$ °C/(W/m²), as specified in AR6 [1] and without feedbacks this gives a basic Equilibrium Climate Sensitivity (temperature increase at doubled CO₂-concentration) of $ECS_B = \lambda_P \cdot \Delta F_{2xCO_2} \approx 1.05$ °C.

Detailed own investigations also show (Harde 2017 [15]) that, different to the IPCC specifications, water vapor only contributes to a marginal positive feedback, and evaporation at the earth's surface even causes a significant negative feedback, yielding an ECS of only 0.7 °C, this in contrast to the last assessment report of the IPCC with 3°C and the Coupled Model Intercomparison Project Phase 6 (CMIP6) with even 3.78°C.

Respective values for CH₄ and N₂O can only indirectly be compared with the literature, as they are only specified for a concentration range (parts per billion) before saturation is observed.

6.5 Note on CH₄

The IPCC lists methane as a gas with a particularly high warming potential. The radiation efficiency of CH₄ with 3.7×10^{-4} W/m²/ppb is classified as 25 times larger than that of CO₂ with 1.4×10^{-5}

W/m²/ppb. Such values are derived from the changing absorptivity or emissivity of the gases when their concentration changes by 1 ppb (part per billion). However, this is based on the fact that two gases are compared under completely different conditions: CH₄ with a concentration of 1.8 ppm and CO₂ with a concentration 200 times higher, when it is already highly saturated. The interference with other greenhouse gases, especially with water vapour, is completely different for both gases and is not taken into account. Only these very different conditions suggest a much higher radiation efficiency of methane.

On the other hand, at a concentration of 400 ppm in the atmosphere or at 10% in the laboratory experiment the radiative efficiency of CH₄ drops to about 75% of the CO₂ value. Only due the different saturation on completely different scales a 25x larger global warming potential is specified for CH₄, while a more realistic scenario by doubling the different actual CH₄, N₂O and CO₂ concentrations shows that CH₄ does not contribute more than about 2% and N₂O only about 1% relative to CO₂ to global warming.

7. Conclusion

To our knowledge we present the first demonstration of the atmospheric greenhouse effect in a laboratory experiment, which also allows quantitative measurements under conditions as in the lower troposphere. We use an experimental set-up consisting of two plates in a closed housing, one plate in the upper position heated to 30°C, the other at the bottom and cooled to -11.4°C. The plates have a distance of 1.11 m to each other, and the tank can be filled with the gases of interest to study the radiation transfer between the plates. This set-up largely eliminate convection or heat conduction and allows to reproducibly study the emission of the GH-gases as additional warming of the heated plate due to back-radiation of the gases. We have investigated the GH-gases carbon dioxide, methane and nitrous oxide as a function of the gas concentration. In addition and independent of the temperature measurements is the back radiation of the GH gases directly recorded as reduced electrical heating of the upper plate.

These measurements clearly demonstrate that contrary to the often misinterpreted 2nd law of thermodynamics a warmer body can further be heated by absorbing the radiation from a colder body, here the radiation from the cooled plate and a GH-gas. They also confirm that GH-gases are still emitting IR-radiation in ‘backward’ direction under conditions as found in the lower atmosphere. The measurements are well confirmed by extensive LBL-RT calculations, which are in full agreement with the recorded temperature and electric heating data, this in absolute numbers and over the whole progression as a function of the gas concentrations. Any noticeable impact in the energy balance due to heat conduction can be excluded by control experiments with noble gases.

At the same time reveal our theoretical studies the principal difficulties to measure the GH-effect as increasing temperature of the gas. More careful examination shows that such trials simply demonstrate heating via absorption of IR or NIR light by the compartment walls and only to some smaller degree by absorption of a gas. But these experiments miss that the greenhouse effect is mainly the result of a temperature difference over the propagation path of the radiation and thus the lapse rate in the atmosphere. A declining GHE with reduced temperature difference between the plates is clearly observed.

From our measurements and their comparison with the calculations we derive the radiative forcing of the gases when doubling their concentrations. This is an important measure to characterise the emissivity of the gases under higher concentration levels, when already stronger saturation on the absorption bands is observed, but it also serves as a relative measure at lower concentrations.

Despite quite different conditions between a laboratory experiment and the real atmosphere the deduced forcings allow some direct comparison with each other. But this requires to consider step by step the different impacts like a changing pressure broadening of the absorption lines over the path-length in the atmosphere, the interference with other GH-gases like water vapor, the different

ground temperature, and the changing back-radiation with varying cloud altitude, overcast and emissivity.

The derived forcing for CO₂ is in quite good agreement with some theoretical studies in the literature, which to some degree is the result of calibrating the set-up to the spectral calculations, but independently it determines and also reproduces the whole progression as a function of the gas concentration. From this we deduce a basic equilibrium climate sensitivity (without feedbacks) of $ECS_B = 1.05^\circ\text{C}$. When additionally assuming a reduced wing absorption of the spectral lines due to a finite collision time of the molecules this further reduces the ECS_B by 10% and, thus, is 20% smaller than recommended by CMIP6 with 1.22°C .

Detailed own investigations also show that in contrast to the assumptions of the IPCC water vapor only contributes to a marginal positive feedback and evaporation at the earth's surface even leads to a significant further reduction of the climate sensitivity to only $ECS = 0.7^\circ\text{C}$ (Harde 2017 [15]). This is less than a quarter of the IPCC's last specification with 3°C (see AR6 [1]) and even 5.4x lower than the mean value of CMIP6 with $ECS = 3.78^\circ\text{C}$

The found forcings for CH₄ and N₂O can only indirectly be compared with the literature, as respective values are only specified for a concentration range (parts per billion) before saturation is observed. Nevertheless their relative values to CO₂ still allow a direct assessment of their contribution to any observed warming, which is not more than 2% for CH₄ and less than 1% for N₂O.

Water vapor as the by far strongest GH-gas in the atmosphere could not be investigated in our set-up. This would require some systematic modifications to realize a similar vapor density profile over the lapse rate as in the atmosphere, and in particular, to avoid condensation at the cold plate. But it would be highly desirable to realize also for this GH-gas quantitative measurements, together with CO₂ as a mixture, to study the interdependence of these gases in their overlapping absorption spectra and by this to collect more reliable data about their impact on our climate. Based on a set-up as presented here but with a further developed equipment, particularly with well stabilized components and an improved temperature recording such investigations would be very helpful for objectification of the further climate debate.

The presented measurements and calculations clearly confirm the existence of an atmospheric GHE, but they also demonstrate the only small impact on global warming, which apparently is much more dominated by natural impacts like solar radiative forcing (see, e.g., Connolly et al. 2021 [16]; Harde 2022 [17]). Therefore, it is high time to stop a further indoctrination of our society with one-sided information, fake experiments, videos or reports, only to generate panic. Instead we have to come back to a consolidated climate discussion, which concentrates on facts and also includes the benefits of GH-gases.

In the long term, an economic shift to new forms of energy generation, of whatever kind, is inevitable, since the supply of fossil fuels is finite. However, there is no need to drive this process blindly and hastily; otherwise there is a risk of deindustrialization, which would then really trigger a dire future for the next generations.

References

1. Sixth Assessment Report (AR6) of the IPCC, 2021: Climate Change 2021: The Physical Science Basis, Contribution of Working Group I to the Sixth Assessment Report of the Intergovernmental Panel on Climate Change [Masson-Delmotte, V. et al. (eds.)]. Cambridge University Press.
2. J. B. Fourier, 1824: *Remarques Générales Sur Les Températures Du Globe Terrestre Et Des Espaces Planétaires*. In: *Annales de Chimie et de Physique*, Vol. 27, 1824, S. 136–167, https://books.google.co.uk/books?id=1Jg5AAAACAAJ&pg=PA136&hl=pt-BR&source=gbs_selected_pages#v=onepage&q&f=false

3. R. W. Wood, 1909: *Note on the Theory of the Greenhouse*, London, Edinburgh and Dublin Philosophical Magazine, Vol. 17, pp. 319-320.
4. T. Allmendinger, 2006: The thermal behaviour of gases under the influence of infrared-radiation, *Int. J. Phys. Sci.* 11: pp. 183-205.
5. N. S. Nahle, 2011: *Repeatability of Professor Robert W. Wood's 1909 experiment on the Theory of the Greenhouse*, Biology Cabinet Online-Academic Resources and Principia Scientific International, Monterrey, N. L.
6. V. R. Pratt, 2020: *Wood's 1909 greenhouse experiment, performed more carefully*, <http://clim.stanford.edu/WoodExpt/>.
7. E. Loock, 2008: *Der Treibhauseffekt - Messungen an einem Wood'schen Treibhaus*, <https://docplayer.org/30841290-Der-treibhauseffekt-messungen-an-einem-wood-schen-treibhaus-von-ehrenfried-loock-version.html>.
8. T. O. Seim, B. T. Olsen, 2020: The Influence of IR Absorption and Backscatter Radiation from CO₂ on Air Temperature during Heating in a Simulated Earth/Atmosphere Experiment, *Atmospheric and Climate Sciences*, 10, pp. 168-185, <https://doi.org/10.4236/acs.2020.102009>.
9. H. v. Dittfurth, 1978: *Studio-Demonstration in German TV*, ZDF TV-Series "Querschnitte".
10. M. Schnell, 2020: *Die falschen Klimaexperimente*, <https://www.eike-klima-energie.eu/2020/11/06/die-falschen-klima-experimente/>.
11. A. Gore, D. Guggenheim, 2006: *An Inconvenient Truth*, Movie, <https://www.imdb.com/title/tt0497116/>.
12. A. Watts, 2011: *Replicating Al Gore's Climate 101 video experiment shows that his "high school physics" could never work as advertised*, <https://wattsupwiththat.com/2011/10/18/replicating-al-gores-climate-101-video-experiment-shows-that-his-high-school-physics-could-never-work-as-advertised/?cn-reloaded=1>.
13. J.-E. Solheim, 2016: *Start des zweitägigen „Al Gore-Experiments“*, 10. Internationale Klima- und Energie-Konferenz (10. IKEK), EIKE, Berlin, <https://www.eike-klima-energie.eu/2017/02/04/10-ikek-prof-em-jan-erik-solheim-start-des-zweitaegigen-al-gore-experiments/>.
14. H. Harde, 2013: *Radiation and Heat Transfer in the Atmosphere: A Comprehensive Approach on a Molecular Basis*, *Intern. Journal of Atmospheric Sciences*, vol. 2013, Article ID 503727, 26 pages, <http://dx.doi.org/10.1155/2013/503727>
15. H. Harde, 2017: *Radiation Transfer Calculations and Assessment of Global Warming by CO₂*, *International Journal of Atmospheric Sciences*, Volume 2017, Article ID 9251034, pp. 1-30, <https://www.hindawi.com/journals/ijas/2017/9251034/>, <https://doi.org/10.1155/2017/9251034>.
16. R. Connolly, W. Soon, M. Connolly, S. Baliunas, J. Berglund, C. J. Butler, R. G. Cionco, A. G. Elias, V. M. Fedorov, H. Harde, G. W. Henry, D. V. Hoyt, O. Humlum, D. R. Legates, S. Luning, N. Scafetta, J.-E. Solheim, L. Szarka, H. van Loon, V. M. V. Herrera, R. C. Willson, H. Yan and W. Zhang, 2021: *How much has the Sun influenced Northern Hemisphere temperature trends? An ongoing debate*, *Research in Astronomy and Astrophysics* 2021 Vol. 21 No. 6, 131(68pp), <http://www.raa-journal.org/raa/index.php/raa/article/view/4906>.
17. H. Harde, 2022: *How Much CO₂ and the Sun Contribute to Global Warming: Comparison of Simulated Temperature Trends with Last Century Observations*, *Science of Climate Change*, vol. 2, no. 1, pp. N1 1-29, <https://doi.org/10.53234/scc20221/28>.